Paper Number 135

DROPWISE CONDENSATION OF LIQUID METAL VAPOUR UNDERNEATH A FLAT INCLINED SUBSTRATE

Basant Singh Sikarwar, Sameer Khandekar* and K. Muralidhar
Department of Mechanical Engineering
Indian Institute of Technology Kanpur, Kanpur 208016, India
*Corresponding Author: Tel: +91 512 259 7038, Fax: +91 512 259 7408, samkhan@iitk.ac.in

ABSTRACT

Although dropwise condensation of metallic vapor underneath a cold substrate is an efficient route for heat transfer that is encountered in many industrial applications, its long term sustainability on common engineering substrates is a challenging task. Quantification of the substrate leaching rate induced by droplet motion requires knowledge of the local heat and momentum transport coefficients. Against this background, the quasi-periodic time cycle of droplet growth, from the minimum drop size to drop slide-off /fall-off, fluid flow and heat transfer inside the drop, wall shear stresses between the condensate and the substrate, and the effective local and average transfer coefficients, are reported in the present study. The evolution of the collection of drops is numerically simulated by solving suitable model equations. Fluid motion and heat transfer inside a single drop are determined from the conservation equations using a finite volume method. Thermophysical properties, as appropriate for metallic vapor and liquid metals (Sodium, Potassium and Mercury) are utilized in the simulation. The critical sizes of the drops at slide-off and fall-off, underneath horizontal and inclined surfaces, are also reported.

NOMENCLATURE

H	Latent heat of vaporization (kJ/kg)
h	Heat transfer coefficient (W/m^2-K)
k	Thermal conductivity (W/m-K)
L	Length (m)
q	Surface heat flux (W/m^2)
r	Radius of drop (m)
T	Temperature (K)
ΔT	Temperature drop (K)
Δt	Time step (s)
u	Velocity (m/s)
U	Velocity of the moving drop (m/s)
V	Volume of the drop (m^3)
P	Pressure (N/m^2)

Greek symbols

α	Inclination angle (deg)
μ	Dynamic viscosity (Pa-s)
v	Specific volume (m^3/kg)
ρ	Density (kg/m^3)
σ	Surface tension of liquid (N/m)
τ	Shear stress (N/m^2)
θ	Contact angle (deg)

Subscripts

adv	Advancing
avg	Average
b	Base
c	Condensate
crit	Critical
d	Drop
g	Gravity
int	Interfacial heat and mass transfer
l	Liquid
lv	Liquid vapor interface
max	Maximum
min	Minimum
rcd	Receding
sat	Saturation
sl	Solid-liquid interface
t	Total
v	Vapor
w	Wall
x, y, z	Cartesian coordinates

INTRODUCTION

It is well known that heat transfer coefficient in dropwise mode of condensation is higher than in the filmwise mode [1-2]. In dropwise condensation, drops grow first by direct condensation and later by coalescence among the neighbors. At a later stage of droplet growth, net body forces exceed the retention force due to surface tension, leading to the sliding of drops and/or eventual fall-off. Portions of the substrate are exposed again and a new cycle of generation, growth and fall-off is commenced. The overall process is cyclic, as observed by various authors [2-4]. The

direct impact of this quasi-periodic cyclic process is an enhancement of the heat transfer coefficient [4-5]. This is beneficial from an energy conservation perspective as the pumping power and consequently the size of the related equipment can be effectively reduced. An example is the consequence of heat transfer enhancement in sodium heat exchangers used in the fast breeder nuclear reactor [6]. The condensing cycle of nucleation, growth and drop removal at criticality can also used in the purification of liquid metals in closed vacuum conditions.

Specially engineered surfaces that promote dropwise condensation of commonly encountered liquids rather than the filmwise mode are achievable by nanotexturing processes, chemical texturing using deposition of mono-layers of organic molecules, and thin film coating technology. Long term sustainability of such physically and chemically textured surfaces is a complex subject because the promoter layer is leached by the shear stresses generated by the sliding drops [5]. Surface leaching is primarily affected by viscous forces at the contact surface and chemical reactions between the condensing liquid and the lyophobic promoter. Heat transfer rates and pressure and temperature fluctuations will also affect the life of the textured surface [5, 7]. Therefore, to estimate the life cycle of surfaces textured by promoter layers, particularly when the material condensing is a heavy metal, it is necessary to model the condensation cycle in as much detail as possible.

Open literature on surface leaching due to motion of liquid drops, metallic and otherwise, is limited. Many of the reported studies have considered the critical state of a sessile drop on an inclined surface with a focus on the contact angle hysteresis, drop shape, and drop retention [8-9]. There are a few studies on the sliding behavior of the drop on an inclined surface. Kim et al. [10] performed experiments for measuring steady sliding velocity of liquid drops on an inclined surface and reported a scaling law to determine the sliding velocity of liquid with known wetting characteristics. Sakai and Hashimoto [11] experimentally determined the velocity vector distribution inside a sliding sessile drop using PIV. The authors reported that the velocity gradient near the liquid-solid interface is higher than locations elsewhere inside a drop. This analysis was further used to recognize the slipping and rolling components of the sliding velocity and the acceleration of the water drop [12]. Das and Das [13] used smooth particle hydrodynamics to numerically simulate the movement of drops down an inclined plane. The study captured the internal circulation inside a sliding sessile drop. It was shown that the frictional resistance by viscosity at the solid-liquid interface cannot be neglected in estimating the sliding behavior. Sikarwar et al. [5] numerically correlated the wall shear stress and wall heat transfer coefficient as a function of Reynolds number and Prandtl number for a water drop sliding at constant speed. With the shear stress and local heat transfer distributions given, the effect of an ensemble of drops can be determined using their population density model. This information is vital for the estimation of surface leaching. Such an analysis, particularly for metallic vapors and liquids is not available in the literature.

In the present work, a mathematical model of heat and momentum transport inside individual condensing drops, as well as the complete simulation of the condensation process below a sub-cooled substrate, is presented. A computer code has been developed to determine the time cycle of growth from the minimum drop size to slide-off /fall-off. Fluid flow and heat transfer inside the drop during its motion, wall shear interactions between the condensate and substrate, and effective local and average transport coefficients are presented for a variety of liquid metals (Na, K and Hg).

MODEL DEVELOPMENT

Atomistic modeling of drop formation in heterogeneous dropwise condensation has been carried out by Sikarwar et al. [5]. The authors reported that the minimum drop radius does not provide controllability of macroscale dropwise condensation at large timescales when dynamic steady-state is achieved. Therefore, drops formed at the initial nucleation site are assigned a minimum possible stable radius from thermodynamic considerations. At the nucleation sites, drops first grow by direct condensation and then by coalescence with the neighboring drops. When a certain drop size is reached, body forces exceed surface tension and the drop is set in motion. In the present work, dropwise condensation is simulated in two parts. The first part describes the simulation of growth of drops underneath an inclined substrate by direct condensation followed by coalescence. This model is derived from the previous work of the authors [2]. In the second part, fluid flow and heat transfer inside a drop sliding on an inclined substrate has been simulated.

Part 1 - Modeling dropwise condensation: Growth of drops is simulated here starting from the postulate that the drop embryos form and grow at specific nucleation sites ($10^9/cm^2$), while the portion of the surface between the growing drops remains essentially ‘dry’. The nucleation sites are randomly distributed on the

substrate. The minimum size of the drop can be found from thermodynamic considerations as [4]

$$r_{\min} = \left(\frac{2\sigma_{lv}}{H_{lv} \cdot \rho \cdot \Delta T} \right) \quad (1)$$

These drops first grow by direct condensation up to a size that is of the order of magnitude of the distance between the neighboring nucleation sites. Beyond this point, coalescence between neighboring drops takes place and the subsequent growth of the drops will occur by a combination of direct condensation and coalescence. The growth rate by direct condensation is given as [2]

$$\frac{dr}{dt} = \left(\frac{4\Delta T_t}{\rho_l \cdot H_{lv}} \right) \cdot \left[\frac{\left(1 - \frac{r_{\min}}{r} \right)}{\left(\frac{2}{h_{\text{int}}} + \frac{r}{k_c} \right)} \right] \cdot \left(\frac{(1 - \cos\theta)}{(2 - 3\cos\theta + \cos^3\theta)} \right) \quad (2)$$

When two drops touch each other, they are replaced by a drop of equal volume, placed at their resultant center of mass. The drops are allowed to grow up to the critical size where the gravity force exceeds the retention force due to surface tension. The drop may then fall-off (for a horizontal substrate) or slide over the inclined substrate. The hidden sites underneath the original drop become active and the process is repeated.

The distance between two nucleation sites, *i* and *j* on the substrate, was calculated by following equation

$$d_{ij} = \sqrt{\left(x_i - x_j \right)^2 + \left(y_i - y_j \right)^2 + \left(z_i - z_j \right)^2} \quad (3)$$

Therefore, the coalescence criterion for the present study is stated as

$$d_{ij} - \left(r_i + r_j \right) < 10^{-3} \quad (4)$$

The size of the drop at fall-off is obtained as [9]

$$r_{\max} = \sqrt{\left(\frac{6\left(\sin^3\theta_{avg} \right)\left(\cos\theta_{rcd} + \cos\theta_{adv} \right)}{\left(2 - 3\cos\theta_{avg} + \cos^3\theta_{avg} \right)\left(\pi - \theta_{rcd} - \theta_{adv} \right)} \right) \cdot \left(\frac{\sigma}{(g \cdot \cos\alpha)(\rho_l - \rho_v)} \right)} \quad (5)$$

The critical size of the drop, at slide-off for an inclined substrate, has been derived by the authors [7] as

$$r_{crit} = \sqrt{\left(\frac{3\sin^3\theta_{avg}}{\pi\left(2 - 3\cos\theta_{avg} + \cos^3\theta_{avg} \right)} \right) \cdot \left[\left(\frac{\pi}{2\pi - \theta_{rcd} - \theta_{adv}} \right) \left\{ \begin{matrix} \sin\left(2\pi - \theta_{rcd} \right) \\ -\sin\theta_{adv} \end{matrix} \right\} + \left(\frac{\pi}{\theta_{adv} + \theta_{rcd}} \right) \left\{ \sin\theta_{rcd} + \sin\theta_{adv} \right\} \right] \cdot \left(\frac{\sigma}{(g\sin\alpha)(\rho_l - \rho_v)} \right)} \quad (6)$$

The terminal velocity of a sliding drop is calculated from a force balance equation. It is experimentally known that the sliding drop sweeps away a large number of drops in its path and creates a bare surface for the next cycle of nucleation. There are two possibilities: (i) fall-off critically is not achieved during the entire slide-off; (ii) fall-off criticality is achieved during sliding motion before the drop traverses the entire length of the substrate. Both of these possibilities have been incorporated in the simulation.

Numerical Algorithm: The important steps of the numerical algorithm are listed here: (i) Initialize all variables and input material properties; (ii) randomly distribute the nucleation sites (10^9/cm^2) on the substrate and place drops of minimum radius at all nucleation sites, respectively; (iii) calculate the intermediate distance between nucleation sites; (iv) solve Equation 2 by a 4th order Runge-Kutta method and find the new radius; (v) check for coalescence; (vi) identify the sites covered by drops and make them hidden; (vii) search for exposed sites and provide a minimum radius drop on such sites; (vii) check for the critical radius of slide-off and the sliding velocity; (viii) check for drop fall-off; (ix) repeat (iii)-(viii) till a quasi-dynamic steady state is reached.

Surface heat flux calculation: Local heat fluxes have been calculated by using a quasi-one dimensional approximation for thermal resistance, including the interfacial resistance at the vapor-liquid boundary and conduction resistance through the local drop height. With a drop size distribution, it is now possible to estimate the total heat transfer over an area and hence the average heat flux. The gaps between drops are assumed to be covered by a thin film of the condensing liquid, which is only postulated to be a few nanometers thick.

Part 2 - Fluid motion within sliding drops: The schematic diagram of a three-dimensional deformed liquid metal drop with an advancing angle θ_{adv} and a receding angle[1] θ_{rcd} is shown in Figure 1. A typical computational domain with a triangular face on the boundary, tetrahedral element inside and the applicable Cartesian coordinate system is shown in Figure 1(b). The frame of reference is the liquid drop, with the wall moving relative to it at constant speed. The shape and volume of the drop are determined by the two-circle approximation [5, 9]. Fluid flow and temperature distribution are obtained by numerically solving the unsteady Navier-stokes equations and energy equations in three dimensions. From this data, the wall shear stress and wall heat transfer coefficient are calculated as

$$\left.\begin{aligned} \tau_{xy} &= \mu\left[\left(\partial u_x / \partial y\right) + \left(\partial u_y / \partial x\right)\right]_{wall} \\ \tau_{zy} &= \mu\left[\left(\partial u_z / \partial y\right) + \left(\partial u_y / \partial z\right)\right]_{wall} \\ \tau &= \sqrt{\tau_{xy}^2 + \tau_{zy}^2} \end{aligned}\right\} \quad (11)$$

$$q = -k\left[\partial T / \partial n\right] = -k\left[\partial T / \partial y\right]_{wall} \quad (12)$$

$$h = q / \Delta T \quad (13)$$

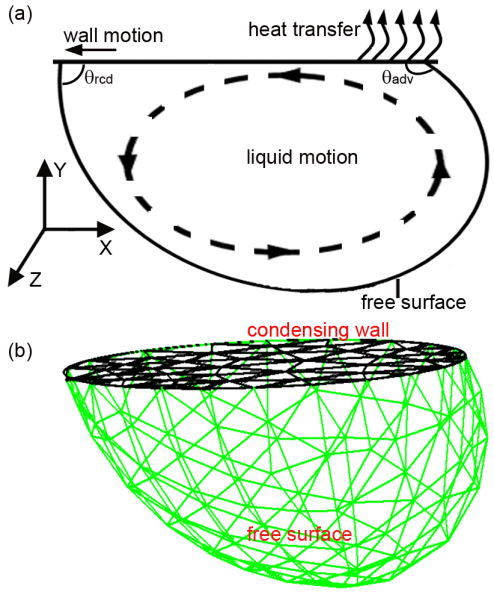

Figure 1

(a) Schematic diagram of fluid motion and heat transfer at the scale of a single drop.

(b) Computational domain with tetrahedral elements in an unstructured grid.

[1] The difference between the advancing and receding angles is called hysteresis whose values used in simulation are given in Table 1.

Numerical methodology: The present simulation is based on finite volume discretization (FVM) of the three dimensional unsteady Navier-Stokes equations over an unstructured mesh. Between vertex-centered and cell-centered placement of variables [14], the pressure correction procedure is cell centered, collocated with the fluid velocities. The unstructured mesh is filled with tetrahedral elements of nearly equal volumes. Pressure-velocity coupling is treated using a smoothing pressure correction method that results in a SIMPLE-like algorithm. Convective terms are discretized by a second order upwind scheme. Geometry invariant features of the tetrahedral element are used so that the calculation of gradients at cell faces is simplified using nodal quantities of a particular variable. Nodal quantities, in turn, are calculated as a weighted average of the surrounding cell-centered values [15]. The diffusion terms are discretized using a 2nd order central-difference scheme.

The discretized system of algebraic equations is solved by the stabilized bi-conjugate gradient method (biCGStab) with a diagonal pre-conditioner. The overall solution algorithm used for the present study is quite similar to that proposed by Date [16]. Points of difference are related to the use of certain invariant properties of the tetrahedral element, powerful linear equations solver as well as a parallel implementation of the computer program. Iterations within the code are run till a convergence in terms of the residual of order 10^{-7} is reached.

RESULTS AND DISCUSSION

Dropwise condensation of sodium, potassium and mercury vapor underneath a substrate inclined at an angle of 10° has been simulated. The condensing surface does not have any preferred texturing except that it promotes dropwise condensation. The details related to the advancing and receding contact angles for each of the metals are given in Table 1. Thermo-physical properties of the liquid metals have been evaluated at the average temperature of the condensate and the substrate.

Table 1
Input parameters used for simulation of metal vapor condensation

Liquid metal	T_s K	T_w K	α deg	θ_{rcd} deg	θ_{adv} deg	θ_{avg} deg	$\Delta\theta$ deg	σ N/m
Na	600	599	10	103	115	108	12	0.17
K	422	421	10	95	105	100	10	0.09
Hg	600	599	10	100	130	115	30	0.42

Table 2
Results of simulation of dropwise condensation of metal vapor

Liquid metal	Radius (mm)			Cycle time (min)	Heat flux (MW/m^2)
	r_{min}	r_{cric}	r_{max}		
Na	6.68×10^{-5}	4.83	6.68	3.85	1.19
K	4.11×10^{-5}	3.52	5.07	2.90	1.01
Hg	1.30×10^{-4}	2.32	2.87	0.75	0. 91

The dropwise condensation cycle reported by various authors, in simulation as well as experiments is reproduced in the present work, Figure 2 [2]. The intermediate steps are initial nucleation, coalescence, slide/fall-off and re-nucleation. The larger drops grow primarily through coalescence because the rate of direct condensation on a larger drop is relatively smaller than on smaller ones. Drop coalescence plays an important role in generating bare areas for re-nucleation. This step is important for deriving higher heat transfer rates through the condensing substrate in dropwise condensation.

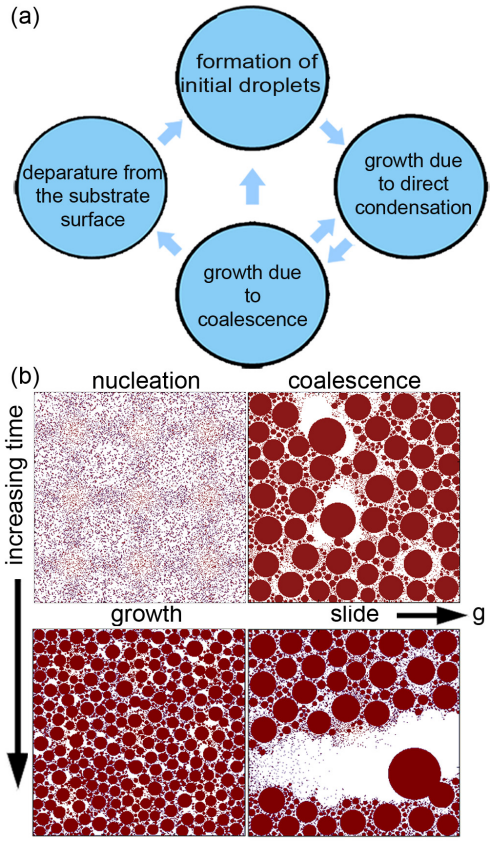

Figure 2
Cycle of individual process observed at various time instants in simulation mercury condensation underneath an inclined substrate. Input parameters for numerical simulation are given in Table 1.

The drop radii at nucleation (r_{min}), slide-off (r_{cric}), and fall-off (r_{max}), apart from the condensing cycle time and heat transfer rates through the substrate are summarized in Table 2. The cycle time is seen to be close to a minute for the metals considered. The maximum drop sizes reached are of the order of a few mm. The critical size of the sodium drop reached just before sliding motion is higher as its high thermal conductivity ensures that it continues growing for a longer duration as compared to mercury and potassium, respectively.

The spatio-temporal drop size distribution and the corresponding distribution of the heat transfer rate underneath a cool substrate for mercury are shown in Figure 3. The drop distribution and heat transfer rate through the substrate is qualitatively compared with a liquid crystal thermography image of condensing water vapor underneath a substrate [7]. Figures 3(a) and 3(b) are camera captured views of condensation and instantaneous experimental substrate temperature profile of condensing water vapor. Figures 3(c) and 3(d) are simulation data of the present work for mercury. The comparison shows similarity in the sense that small heat fluxes are obtained under the foot-print of larger drops.

Soon after a drop is nucleated, the heat transfer rate is high, diminishing as the size of the drop increases. For a drop grown by vapor condensation as well as coalescence, the maximum heat transfer rate appears near the contact line. The thickness of the drop here is the lowest, indicating lower thermal resistance. The central portion of the drop has a higher thermal resistance and therefore a lower heat transfer per unit area. Immediately circumscribing the apparent contact line of the pendant drop, the thin condensate liquid film ensures lower thermal resistance to heat transfer through it. These results explain why the cycle of drop formation, growth and fall-off ultimately enhance the heat transfer rate.

Figure 4 shows the variation in the critical angle of inclination of the substrate for the commencement of droplet sliding as a function of the drop radius, for various simulated liquid metals. The drop fall-off sizes for a horizontal substrate are approximately equal for the three metals. Larger differences are to be seen in the critical radii among the three metals for an inclined surface. These are also smaller than the drop size at fall-off. At criticality, it is clear that drops would first slide away on an inclined surface. Thus, the cycle time is reduced and there is a further increase in the heat transfer rate.

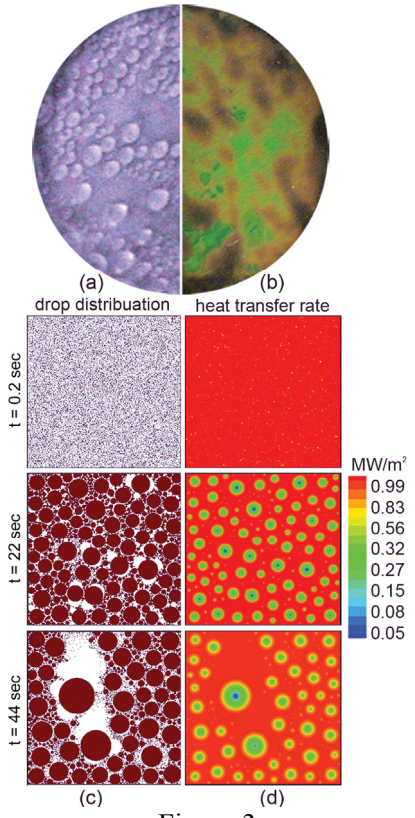

Figure 3

(a) Experimentally recorded drop distribution for condensation of water vapor; (b) Instantaneous liquid crystal thermograph of the substrate [7]; (c-d) Simulation data of condensation of mercury (left) and heat transfer rates at various time instants (right).

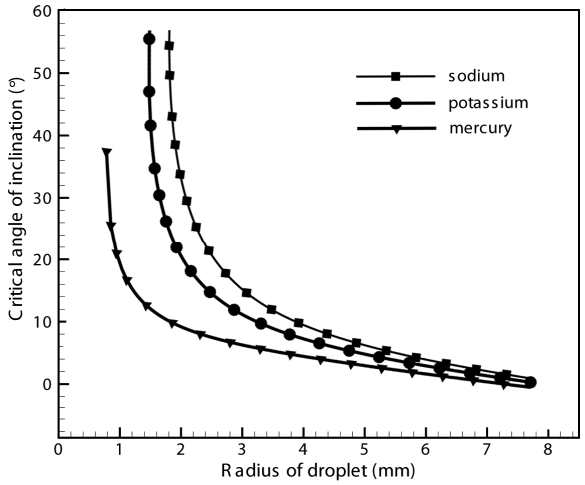

Figure 4

Critical angle of inclination of the substrate as a function of drop size with respect to fall-off (horizontal substrate) and slide-off (inclined substrate).

To determine the rate of leaching of a substrate and improvement of heat transfer due to sliding of drop, velocity and temperature fields are required. The simulation based on the Navier-Stokes equations are presented in the form of streamlines, velocity contours, wall pressure, wall shear stress, temperature contours and heat transfer coefficient.

Figure 5 shows the streamlines and the dimensionless velocity contours at various Reynolds number for liquid sodium. At a higher Reynolds number, the streamline density is higher near the solid wall. The velocity magnitude near the free surface is close to the wall speed, in the opposite direction. The local pressure and shear stress distribution at the wall of condensing liquids (sodium, potassium and mercury) are shown in Figures 6(a) and 6(b). The maximum wall pressure and shear stress appear at the contact line of the drop. It can be concluded from this data that the highest substrate damage can be expected near the contact line when compared to the center. The average wall shear stress and heat transfer coefficient are given in Table 3 below.

Table 3

Average wall shear stress and heat transfer coefficient as a function of Re and Pr

Liquid metal	Re	Average wall shear stress (N/m^2)	Average heat transfer coefficient (W/m^2 K)
Sodium (Pr = 0.005)	0	0	8.32×10^4
	10	1.58×10^{-4}	8.39×10^4
	50	7.96×10^{-4}	8.46×10^4
	100	1.62×10^{-3}	8.69×10^4
Potassium (Pr = 0.007)	0	0	4.632×10^4
	10	1.323×10^{-4}	4.669×10^4
	50	7.845×10^{-4}	4.8345×10^4
	100	1.592×10^{-3}	4.9657×10^4
Mercury (Pr = 0.011)	0	0	9.82×10^3
	10	2.945×10^{-4}	9.91×10^3
	50	1.547×10^{-3}	1.05×10^4
	100	3.69×10^{-3}	1.56×10^4

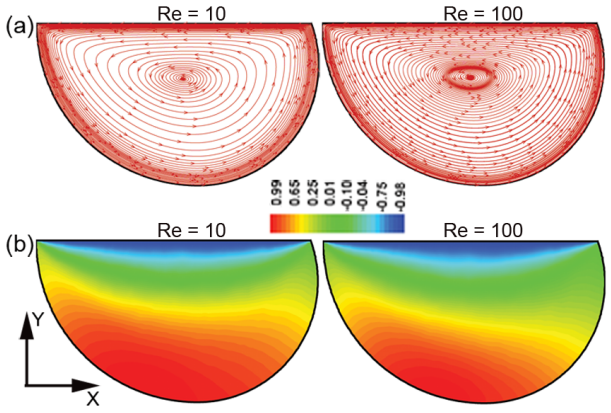

Figure 5

(a) Streamlines show the motion of the liquid inside the sliding drop (b) Contours of the dimensionless velocity on the plane considered in (a).

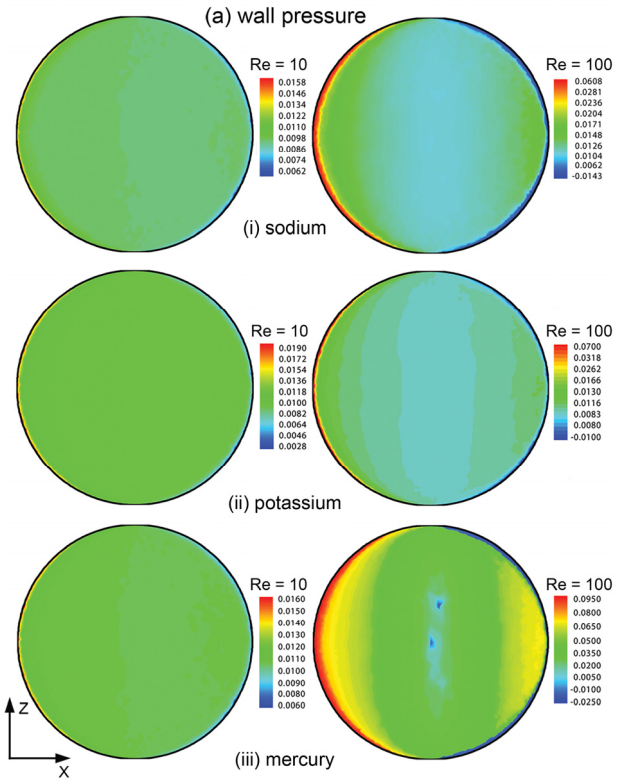

Figure 6

(a) Local wall pressure distribution and (b) local wall shear stress contours at Re = 10 and 100 for various liquid metals (Na, K and Hg).

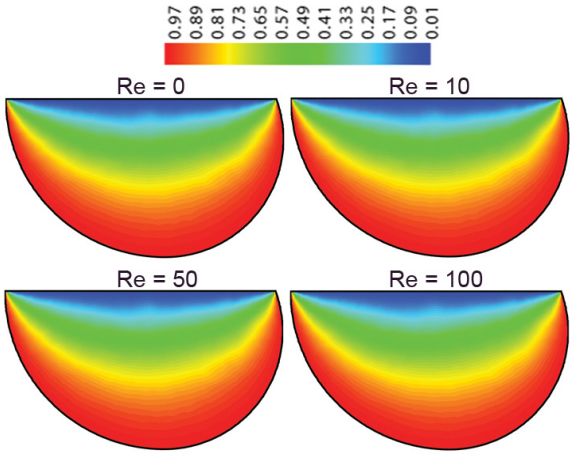

Figure 7

Non-dimensional temperature contours of liquid sodium at various Reynolds numbers.

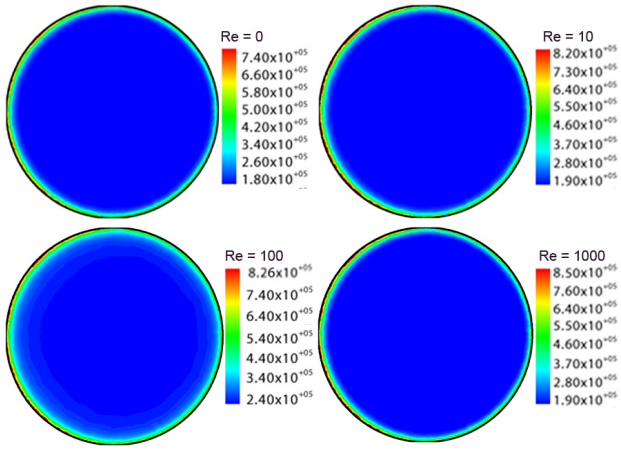

Figure 8

Wall heat transfer coefficient distribution for liquid sodium at various Reynolds numbers.

Figure 7 show the temperature field within the drop of liquid sodium for various Reynolds number. The changes in the temperature field arising from the velocity field are barely seen in theses contours. Hence, the non-dimensional temperature contours confirm that heat transfer is predominantly by conduction. Figure 8 show that heat transfer coefficient slightly increases as the Reynolds number increases, but the change is quite small. These data for the metals studied are summarized in Table 3.

CONCLUSIONS

A detailed simulation of dropwise condensation and simulation of fluid flow and heat transfer inside a sliding liquid drop has been carried for a surface inclined at an angle of 10° with the horizontal. The condensing drop is taken to be liquid metal. Various processes in dropwise condensation and corresponding

heat flux distribution with respect to time and space have been presented. The quasi-periodicity and cyclical nature of dropwise condensation is mainly responsible for the enhancement of the heat transfer coefficient in dropwise condensation. On other hand, information on fluid flow and heat transfer inside the sliding drop is needed to estimate the shear stress patterns over the substrate. Estimation of the leaching rates is important in many engineering applications, for example (a) estimation of life cycle of a heat exchanger textured by promoter layers and (b) estimation of substrate life on which heavy liquid metals are being deposited under closed vacuum conditions. The simulations of the present work show that shear stress is the greatest at the periphery of the drop. In addition, heat transfer is dominated by heat conduction and larger drops offer greater thermal resistance per unit area.

KEYWORDS
Dropwise condensation, simulation, wall shear stress, heat transfer, liquid metal

ACKNOWLEDGMENT

Financial assistance provided by the Board of Research in Nuclear Sciences, Mumbai (India) is gratefully acknowledged.

REFERENCES

1. Leach, R. N., Stevens F., Langford, S. C., and Dickinson, J. T., 2006, Dropwise Condensation: Experiments and Simulations of Nucleation and Growth of Water Drops in a Cooling System, Langmuir, **22**, pp. 8864-8872.
2. Sikarwar, B. S., Battoo, N. K., Khandekar, S., and Muralidhar, K., 2011, Dropwise Conden-sation underneath Chemically Textured Surfaces: Simulation and Experiments, ASME J. Heat Transfer, **133 (2)**, pp. 021501 (1-15).
3. Vemuri, S., and Kim, K. J., 2006, An Experimental and Theoretical Study on the Concept of Dropwise Condensation, Int. J. Heat Mass Transfer, **49**, pp. 649-857.
4. Carey, V. P., 1992, *Liquid–Vapor Phase–Change Phenomena*, 2nd ed., pp. 342-351, Hemisphere Publishing Corp., New York.
5. Sikarwar, B. S., Khandekar, S., Agrawal, S., Kumar, S. and Muralidhar, K., 2012, Dropwise Condensation Studies on Multiple Scales, Heat Transfer Engineering, Special Issue: Advances in Heat Transfer, **33 (3/4)** (in press).
6. Tanasawa, I., 1991, Advance in Condensation Heat Transfer, in- Advances in Heat Transfer (ed.: Hartnett, J. P., Irvine, T. F., and Cho, I. Y.), **21**, pp. 57-59.
7. Bansal, G. D., Khandekar, S., and Muralidhar, K., 2009, Measurement of Heat Transfer during Dropwise Condensation of Water on Polyethylene, Nanoscale Microscale Thermophy. Engineering, **13**, pp. 184-201.
8. Dussan, E. B., 1985, On the Ability of Drops or Bubbles to Stick to Non-horizontal Surface of Solids, J. Fluid Mech., **151**, pp. 1-20.
9. Elsherbine, A. I., and Jacobi, A. M., 2006, Retention Forces and Contact Angles for Critical Liquid Drops on Non-horizontal Surfaces, J. Colloid and Interface Sci., **299**, pp. 841-849.
10. Ho-Young Kim, Lee, H., and Kang, B. H., 2002, Sliding of Drops Down an Inclined Solid Surface, J. Colloid Sci., **247**, pp. 372-382.
11. Sakai, M. and Hashimoto, A., 2007, Image Analysis System for Evaluating Sliding Behavior of a Liquid Drop on a Hydrophobic Surface, Rev. Scientific Instruments, **78**, pp. 045105-045109.
12. Sakai, M., Song, J., Yoshida, N., Suzuki, S., Kameshima Y. and Nakajima, A., 2006, Direct Observation on Internal Fluidity in a Water Drop during Sliding on Hydrophobic Surfaces, Langmuir, **22**, pp. 4906-4909.
13. Das, A. K., and Das, P. K., 2009, Simulation of Drop Movement over an Inclined Surface using Smoothed Particle Hydrodynamics, Langmuir, **25**, pp. 11459-11466.
14. Barth, T. J., and Jespersen, D. C., 1989, The Design and Application of Upwind Schemes on Unstructured Meshes, AIAA-89-0366, **89**.
15. Frink, N. T., Paresh, P., and Shahyar, P., 1991, A Fast Upwind Solver for the Euler Equations on Three Dimensional Unstructured Meshes, AIAA-91-0102, **91**.
16. Date, A. W., 2005, Solution of Transport Equations on Unstructured Meshes with Cell Centered Collocated Variables. Part I: Discretization, Int. J. Heat Mass Transfer, **48**, pp. 1117-1127.